Available online at www.sciencedirect.com
SCIENCE DIRECT®
International Journal of Heat and Fluid Flow 24 (2003) 122–129
International Journal of HEAT AND FLUID FLOW
www.elsevier.com/locate/ijhff

Linear stability of inverted annular gas–liquid two-phase flow in capillaries

J.-H. Yan, T.S. Laker, S.M. Ghiaasiaan *

The George W. Woodruff School of Mechanical Engineering, Georgia Institute of Technology, Atlanta, GA 30332-0405, USA

Received 30 November 2001; accepted 2 July 2002

Abstract

Linear stability of creeping inverted-annular gas–liquid two-phase flow (liquid core and gaseous annular film) in microtubes, where buoyancy effect is suppressed by surface tension, is addressed. Using a long-wave linear stability solution [Physics of Fluids 14 (1971) 251], the flow field is shown to be linearly unstable for long-wavelength axisymmetric disturbances. The flow field approaches a neutrally stable state as the gas film thickness approaches zero, and instability is enhanced as the phasic velocities are reduced. A two-dimensional linear-stability analysis is also performed in order to examine the stability characteristics at the limit of zero phasic velocities. The analysis leads to a dispersion relation that results in an expression for the neutral wavelength that coincides with the prediction of the Kelvin–Helmholtz stability theory. The neutral and fastest-growing wavelengths are shown to be relatively insensitive to the liquid viscosity.

Keywords: Interfacial waves; Linear stability; Microtubes; Core-annular flow

1. Introduction

The objective of this investigation was to examine the instability due to capillary waves of creeping flow in microtubes when a lubricating thin gas film separates the liquid from the microtube surface. The creeping flow of liquids through capillaries can be obtained with significantly lower pressure drops if an inverted-annular flow pattern can be maintained. Creeping flow of liquids through micropores occurs, and is of interest, in the electrode assemblies of proton exchange membrane (PEM)-based fuel cells. In the gas diffuser, and in the electrode components of the latter assemblies where electrochemical processes leading to the oxidation or reduction of ions take place, liquid water and gas are both present. For effective operation, most current PEM's need to be maintained hydrated, but not flooded, and need careful water management. The problem studied here is also of interest to boiling and two-phase flow in microchannels, since the applicability to microchannels, of the linear interfacial stability methods previously used for modeling and correlation of gas–liquid two-phase phenomena, is questionable. This is due to the predominance of surface tension in microchannels, and due to the fact that the important wavelengths predicted by these methods are typically much larger than the microchannels diameter. The following criterion for the rendition of buoyancy insignificant, suggested by Suo and Griffith (1964), appears to agree with recent experimental studies well (Ghiaasiaan and Abdel-Khalik, 2001), and is used for the definition of microtubes here (Ghiaasiaan and Abdel-Khalik, 2001):

$$R < 0.15L \tag{1}$$

where L is the Laplacian length scale:

$$L = \left[\frac{\sigma}{g(\rho_L - \rho_G)}\right]^{1/2} \tag{2}$$

The stability of the core-annular flow regime associated with the flow of two liquids with unequal but comparable viscosities and densities has been extensively studied in the past, and among the published studies are (Hickox, 1971; Preziosi et al., 1989; Hu and

* Corresponding author. Tel.: +1-404-894-3746; fax: +1-404-894-8496.
E-mail address: seyed.ghiaasiaan@me.gatech.edu (S.M. Ghiaasiaan).

0142-727X/02/$ - see front matter © 2002 Elsevier Science Inc. All rights reserved.
PII: S0142-727X(02)00196-0

Nomenclature

a	dimensionless parameter
A_G, A_L, B_L	wave amplitudes
C	dimensionless wave velocity
d	dimensionless parameter defined in Eq. (8)
D	parameter defined in Eq. (7)
$\mathbf{f}$	function in gas perturbation velocity
$\mathbf{F}$	function in liquid perturbation velocity
g	gravitational acceleration
$\mathbf{g}$	function in gas perturbation velocity
$\mathbf{G}$	function in liquid perturbation velocity
H	dimensionless gas film thickness
h	gas film thickness
K	dimensionless wave number
k	wave number
L	Laplace length scale
m	wave growth parameter
M	gas-to-liquid viscosity ratio
P	pressure
$\mathbf{P}$	function in pressure perturbation
ΔP_σ	capillary pressure
r	radial coordinate
$\mathbf{r}$	dimensionless radial coordinate
R	radius
R_j	jet radius
Re_{L0}	Reynolds number defined in Eq. (16)
t	Time
$u^0_{L,C}$	primary liquid velocity on the centerline
u, v	velocities in axial and vertical directions
x, y	Cartesian (plane) coordinates
$\mathbf{z}$	dimensionless axial coordinate

Greeks

α	dimensionless wave number defined as $k(R-h)$
κ	dimensionless parameter
λ	wavelength
μ	viscosity
ν	kinematic viscosity
ρ	density
σ	surface tension
τ	dimensionless time
ϕ	velocity potential
ψ	stream function
Ω	dimensionless wave growth parameter
ω	wave growth parameter

Subscripts

cr	neutral wavelength
d	faster growing wavelength
G	gas
L	liquid
0, 1	first and second approximations

Superscripts

–	average
0	ideal flow
*	dimensionless
′	perturbation

Joseph, 1989; Frenkel et al., 1987; Aul and Olbricht, 1990; Joseph and Renardy, 1993; Boomkamp and Miesen, 1997; Li and Renardy, 1999; Kerchman, 1995). The investigation by Aul and Olbricht (1990), for example, addressed the stability of annular flow in capillaries under low flow conditions, and included experiments using water as the core fluid, and three polyalkylene glycols as the annular film. The oils had densities close to water, but their viscosities were significantly higher. The experiments showed that the films were unstable under all test conditions. These studies were primarily motivated by oil transportation in pipelines and oil recovery from partially depleted oil fields. The less viscous fluid in the core-annular regime occupies the near-wall high-shear region thereby acting as a lubricant. A good review and classification of the available models for core-annular flow stability, prior to 1995, based on the kinetic energy of the disturbances (Boomkamp and Miesen, 1997), indicates that most of these models have actually addressed viscosity-induced instability. The stability of inverted annular flow in large vertical round tubes has also been studied experimentally (DeJarlais, 1983), and analytically based on the two-fluid modeling technique (Kawaji and Banerjee, 1987).

Hickox (1971) performed a linear stability analysis of core-annular flow in round tubes for long-wavelength disturbances. He showed that, for axisymmetric disturbances when the thinner fluid is at the core, the flow field can be linearly stable only over certain ranges of $(R-h)/R$ (windows of stability). Following Hickox, Joseph et al. (1984) examined the stability of core-annular flow of two immiscible fluids with different viscosities but equal densities, when the considerably more viscous fluid constitutes the core flow. They noted that while flows with the less viscous fluid in the core are unstable to long-wavelength disturbances, the flow field is stable when a thin film of the less viscous fluid constitutes the annular phase.

No systematic analysis or experimental investigation have been reported in the past for the case of core annular flow in microtubes where gravitational effect is suppressed by surface tension, and the annular thinner fluid (gas) also is significantly less dense than the core fluid. The analytical study presented in this paper is meant to elucidate some basic interfacial stability characteristics of microchannels, and show the need for relevant experimental investigations.

It should be mentioned that the stability of a cylindrical jet issuing in an infinitely large gaseous medium could be considered as a crude approximation to the problem of interest here. The linear stability of such jets has been extensively studied long ago (Lamb, 1932; Levich, 1962). Considering symmetrical deformations for common, low-viscosity liquids, these jets are unstable with respect to waves that satisfy $\lambda > 2\pi R_j$, with R_j representing the jet radius. The fastest growing wavelength for these jets, first obtained by Rayleigh in 1878, follows $\lambda_d = 9.016R_j$.

2. Theory

2.1. Long-wavelength stability analysis

The linear stability analysis of Hickox (1971) for axisymmetric perturbations is utilized here. The analysis of Hickox (1971) addresses long-wave axisymmetric as well as asymmetric perturbations. However, since the forthcoming results show that the system is unstable to axisymmetric perturbations under all conditions of interest, asymmetric perturbations need not be considered. Only a brief outline of the theory, as applied in this paper, will be provided. The details can be found in Hickox (1971).

Fig. 1 is a schematic of the flow field. Steady-state, laminar, co-current ideal inverted annular flow, with both phases incompressible, constitutes the primary (undisturbed) flow field. The solution of the Navier–Stokes equations for the primary flow can be represented as:

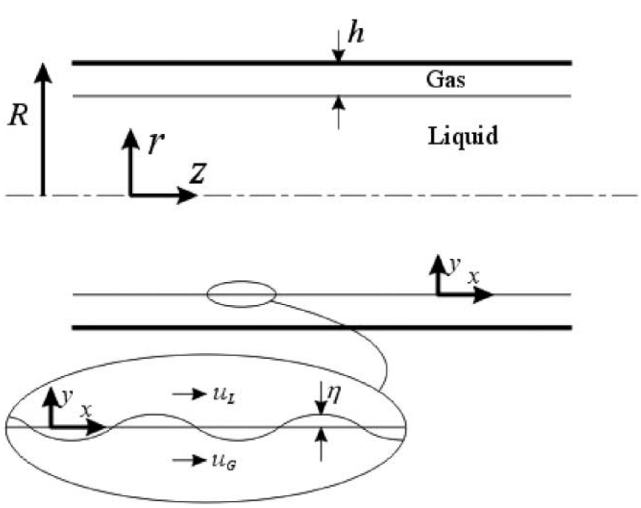

Fig. 1. Schematic of the flow field.

$$\frac{u_L^0}{u_{L,C}^0} = a\mathbf{r}^2 + 1 \tag{3}$$

where $u_{L,C}^0$ is the velocity on the axis of symmetry, and

$$\mathbf{r} = \frac{r}{(R-h)} \tag{4}$$

$$a = \frac{M}{D-M} \tag{5}$$

$$M = \frac{\mu_G}{\mu_L} \tag{6}$$

$$D = \kappa(1-d^2) - 2(1-\kappa)\ln d \tag{7}$$

$$d = (1-H)^{-1} \tag{8}$$

where $\kappa = 1$ when the gravitational effect is negligible.

To examine the effect of small disturbances on the primary flow field, the liquid core is disturbed by the following axisymmetric velocity perturbations:

$$(u', v') = \{\mathbf{F}(\mathbf{r}), i\mathbf{G}(\mathbf{r})\}\exp[i\alpha(\mathbf{z} - C\tau)] \tag{9}$$

$$\frac{P'}{\rho_L} = (u_{L,C}^0)^2\mathbf{P}(\mathbf{r})\exp[i\alpha(\mathbf{z} - C\tau)] \tag{10}$$

where **F**, **G**, and **P** are dimensionless function; α and C are dimensionless wave number and velocity, respectively; and the dimensionless axial coordinate and time, respectively, are defined as:

$$\mathbf{z} = \frac{z}{(R-h)} \tag{11}$$

$$\tau = \frac{u_{L,C}^0 t}{(R-h)} \tag{12}$$

Velocity perturbations similar to Eq. (9), with **F** and **G** replaced with **f** and **g**, respectively, are also imposed on the gaseous phase. The wave velocity C is complex in general, and the sign of its imaginary part determines the flow stability.

A method of regular perturbations around $\alpha = 0$ (corresponding to long wavelengths) is now performed (Lin, 1955; Yih, 1967), whereby (Hickox, 1971):

$$[\mathbf{F}, C] = [\mathbf{F}_0, C_0] + [\mathbf{F}_1, C_1]\alpha + \cdots \tag{13}$$

$$[\mathbf{G}, \mathbf{P}] = [\mathbf{G}_1, \mathbf{P}_1]\alpha + \cdots \tag{14}$$

Functions $\mathbf{f}(\mathbf{r})$ and $\mathbf{g}(\mathbf{r})$ are perturbed similarly. These perturbations are based on the assumption that:

$$\alpha Re_{L0} \ll 1 \tag{15}$$

where

$$Re_{L0} = 2u_{L,C}^0\frac{(R-h)}{\nu_L} \tag{16}$$

The analysis, which is lengthy, is a modification of the analysis of Hickox (1971) and will not be repeated here.

It leads to systems of algebraic equations that should be solved to obtain C_0 and C_1. The first-approximation wave velocity C_0 is always positive and does not cause instability. The second-approximation wave velocity, C_1, on the other hand, is imaginary, and the primary flow is unstable, neutrally stable, or stable, when C_1/i is positive, equal to zero, or negative, respectively.

2.2. Stability analysis for negligibly small axial phasic velocities

The linear stability characteristics in the limit of zero phasic velocities are now addressed. When both phases are inviscid the following expression can be derived by modifying the dispersion relation of a planar interface (Lamb, 1932; Levich, 1962) to include the tangential surface tension force in the interfacial force balance as depicted in the forthcoming Eq. (17):

$$\frac{\omega}{k} = \frac{\rho_L u_L + \rho'_G u_G}{\rho_L + \rho'_G} \pm \left[-\frac{\rho_L \rho'_G}{(\rho_L + \rho'_G)^2}(u_L - u_G)^2 + \frac{\sigma k}{\rho_L + \rho'_G} - \frac{\sigma}{k(R-h)^2(\rho_L + \rho'_G)} \right]^{1/2} \tag{17}$$

where the finite-thickness of the vapor film is accounted for by:

$$\rho'_G = \rho_G \coth(kh) \tag{18}$$

The system becomes unstable when ω/k has an imaginary component, and when u_L and u_G approach zero the neutral disturbances have the familiar Rayleigh wavelength:

$$\lambda_{cr} = 2\pi(R-h) \tag{19}$$

Viscous forces, however, can be significant in microscale. The effect of the liquid viscosity is examined by the simple linear-stability analysis briefly described below.

In the microtube depicted in Fig. 1 the film thickness, h, is assumed to be finite, but sufficiently small compared with channel radius, R, such that a planar two-dimensional analysis can be justified (Gauglitz and Radke, 1988). The viscosity of the gas is assumed to be negligible, and the flow field is assumed to be axisymmetric. The stability analysis is based on the periodic motion of the interface (Lamb, 1932; Levich, 1962), modified to account for the circumferential curvature (Dhir and Lienhard, 1973). Briefly, the liquid and gas mass continuity, and planar momentum equations (in x, y coordinates) are considered in accordance with the small-slope approximation method (Gauglitz and Radke, 1988). The ideal and viscosity-induced velocity components are then represented by the following potential and stream functions, respectively:

$$\Phi_G = A_G \cosh[k(y+h)] e^{\omega t} \cos kx \tag{20}$$

$$\Phi_L = A_L e^{-ky+\omega t} \cos kx \tag{21}$$

$$\psi_L = B_L e^{-my+\omega t} \sin kx \tag{22}$$

Eqs. (21) and (22) satisfy the condition of vanishing viscosity-induced velocities at $y \to \infty$, and are evidently applicable for infinitesimally small interfacial disturbance amplitudes. These functions are now utilized in a linear stability analysis using the following conditions at the interface: equal phasic velocities in the y direction, zero interfacial shear stress (due to negligible gas phase viscosity), and:

$$-P_L + 2\mu_L\left(\frac{\partial u_L}{\partial y}\right) = -P_G - \sigma\frac{\partial^2 \eta}{\partial x^2} - \Delta P_\sigma \tag{23}$$

where the term ΔP_σ, which is de-stabilizing, is the surface tension force caused by the curvature of the channel:

$$\Delta P_\sigma = \frac{\sigma}{R-h} - \frac{\sigma}{R-h-\eta} \approx \frac{\sigma}{R-h}\left(1 + \frac{\eta}{R-h}\right) \tag{24}$$

Eqs. (23) and (24) retain the cylindrical geometry of the interface in accordance with the small-slope approximation (Gauglitz and Radke, 1988; Dhir and Lienhard, 1973), which applies when $|\partial\eta/\partial x| \ll 1$ (Gauglitz and Radke, 1988). The analysis leads to the following dispersion equation:

$$[\rho^* \coth(R^* K H) + 1]\Omega^2 - \frac{K}{R^{*2}(1-H)^2} + K^3 + 4K^4\left[1 - \left(1 + \frac{\Omega}{K^2}\right)^{1/2}\right] + 4\Omega K^2 = 0 \tag{25}$$

where $\rho^* = \rho_G/\rho_L$; $H = h/R$; $R^* = R\sigma/(\rho_L v_L^2)$; $K = k(\sigma/(\rho_L v_L^2))^{-1}$; $\Omega = \omega(\rho_L^2 v_L^3/\sigma^2)$. For the derivation of the non-dimensional parameters R^*, K and Ω, the reference length and time scales were $\mu_L^2/\rho_L\sigma$ and $\mu_L^3/\sigma^2\rho_L$, respectively, which are obtained based on dimensional analysis using the relevant liquid properties, and excluding gravity. The reference length scale is consistent with the way a dimensionless surface tension parameter is defined when strong dependence on velocity and shear rate is avoided, and is evidently appropriate for the analysis presented here. The quantity R^{*-1} is in fact the definition of a surface tension parameter that does not depend on velocity (Preziosi et al., 1989). The interface is evidently unstable when $\Omega > 0$. The neutral condition occurs when $\Omega = 0$, and results in the Rayleigh wavelength, Eq. (19). The neutral wavelength, thus does not depend on liquid viscosity. A similar result has been obtained in the Taylor stability analysis of film boiling of viscous liquids on cylinders (Dhir and Lienhard, 1973). The fastest growing wavelength, Ω_d, occurs when $d\Omega/dK = 0$, whereby:

$$\left(\frac{\rho^* R^* H}{\sinh^2(R^* K H)}\right)\Omega_{\mathrm{d}}^2 - 4K\left[2+\left(1+\frac{\Omega_{\mathrm{d}}}{K_{\mathrm{d}}^2}\right)^{-1/2}\right]\Omega_{\mathrm{d}} - 16K_{\mathrm{d}}^3\left[1-\left(1+\frac{\Omega_{\mathrm{d}}}{K_{\mathrm{d}}^2}\right)^{1/2}\right] - 3K_{\mathrm{d}}^2 = 0 \qquad (26)$$

When $R^* \to \infty$, in the absence of gravity, the system remains linearly stable for all disturbance wavelengths.

3. Results and discussion

3.1. Long-wavelength disturbances

Illustrative parametric calculation results obtained from the numerical solution of the equations described in Section 2.1 are presented in this section. Due to the large number of the physical parameters, representative parametric calculations are presented based on the properties of Refrigerant 134a at equilibrium with its vapor at 1 bar. Extensive other parametric calculations have shown trends similar to those described, however.

Figs. 2–4 display the effects of vapor film-thickness, the liquid Reynolds number, Re_{L0}, and the tube diameter on the disturbance velocity C_1. Note that positive C_1/iRe_{L0} implies an unstable flow. Evidently, the flow field is linearly unstable. Unstable flow was in fact observed in all parametric calculations. The following trends, which are also supported by all the performed parametric calculations, can be noted in the figures. Reducing the tube size, and decreasing Re_{L0} both enhance instability, while the effect of film thickness on C_1/Re_{L0} is not monotonic. Figs. 3 and 4 also depict the effects of liquid viscosity and density, respectively. In Fig. 3 model predictions for saturated R-134a liquid–vapor mixture are compared with results obtained by parametrically increasing and decreasing the liquid viscosity by factor of 2. A similar comparison is depicted in Fig. 4, where the effects of increasing and decreasing the liquid density by factor of 2 are examined. Increasing the viscosity ratio $\mu_{\mathrm{L}}/\mu_{\mathrm{G}}$, and increasing the density ratio $\rho_{\mathrm{L}}/\rho_{\mathrm{G}}$ both enhance instability. The effects of increasing and decreasing the surface tension by factor of 10, furthermore, are depicted in Fig. 5, and show the destabilizing effect of surface tension. All the parametric calculations, however, show that linearly stable flow field with respect to long wavelength disturbances would occur only at the limits of $H \to 0$.

Previously reported studies dealing with core-annular flow, when the phasic densities and/or viscosities are comparable, have shown that stable flow fields can be obtained at least for some parameter ranges (Hickox, 1971; Preziosi et al., 1989). Our analysis, however, indicates that the inverted-annular flow regime in microtubes is generally linearly unstable with respect to long wavelength disturbances.

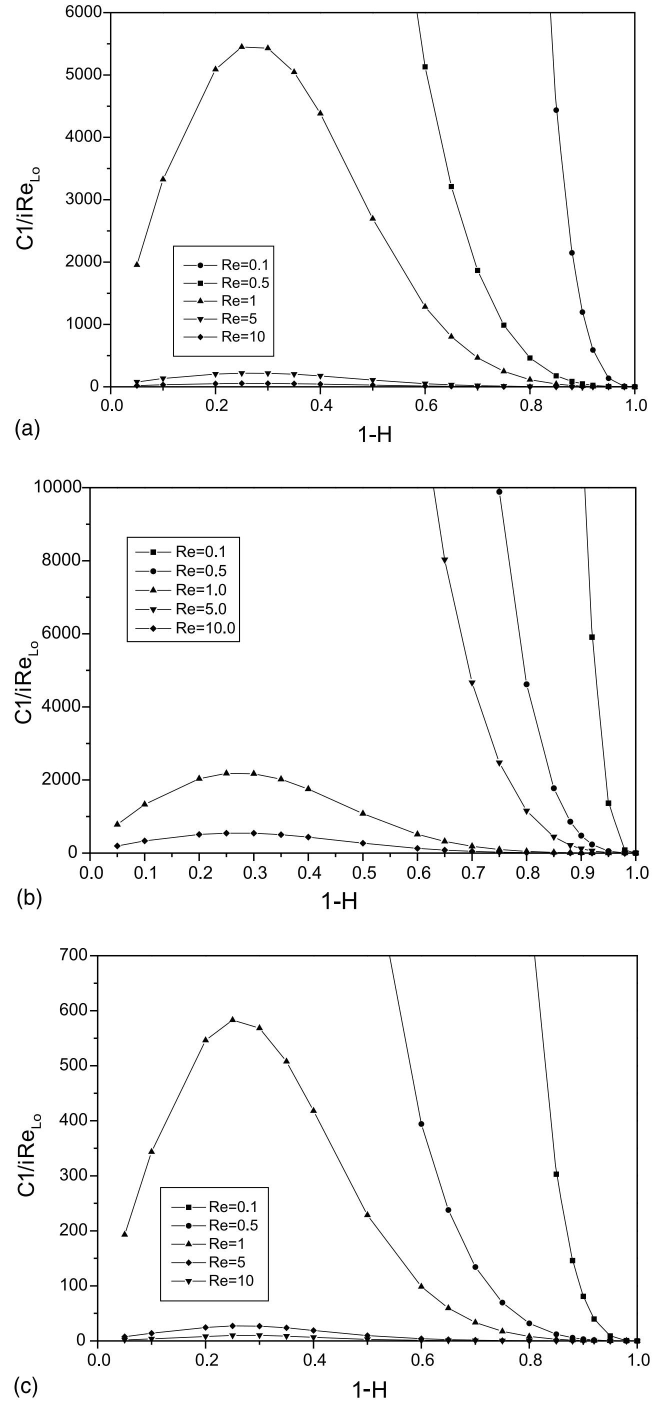

Fig. 2. Long-wavelength disturbance wave velocities: effects of film thickness and liquid Reynolds number. (a) $R = 0.1$ mm, R-134a (b) $R = 1$ mm, R-134a.

3.2. Negligible phasic velocities

Illustrative parametric solutions of Eq. (25) are depicted in Fig. 6(a) and (b), for $R^* = 10^4$ and 10^6,

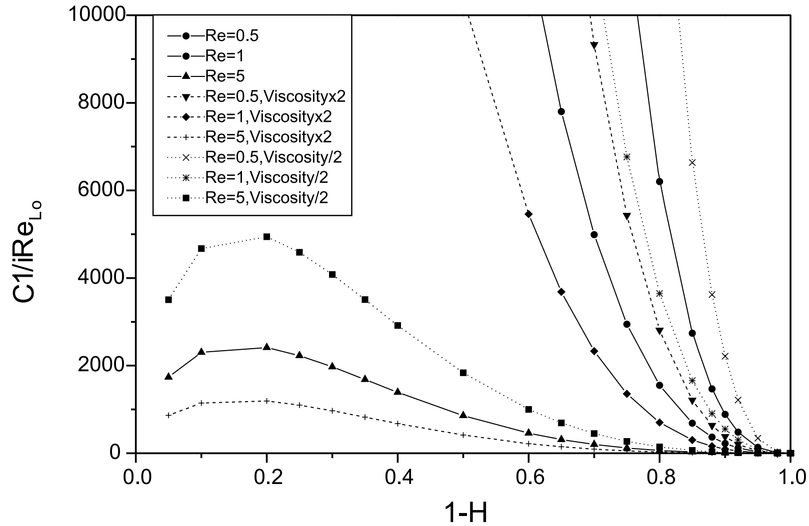

Fig. 3. Long-wavelength disturbance wave velocities: effects of liquid viscosity ($R = 0.25$ mm; R-134a).

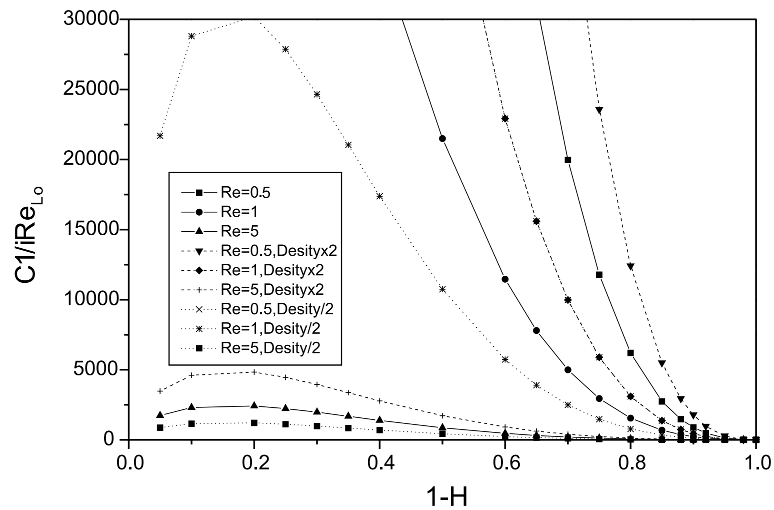

Fig. 4. Long-wavelength disturbance wave velocities: effects of liquid density ($R = 0.25$ mm; R-134a).

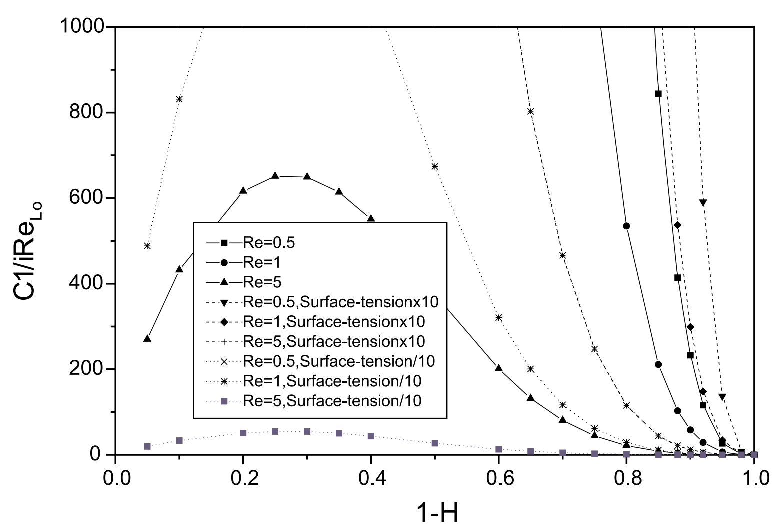

Fig. 5. Long-wavelength disturbance wave velocities: effects of surface tension ($R = 0.25$ mm; R-134a).

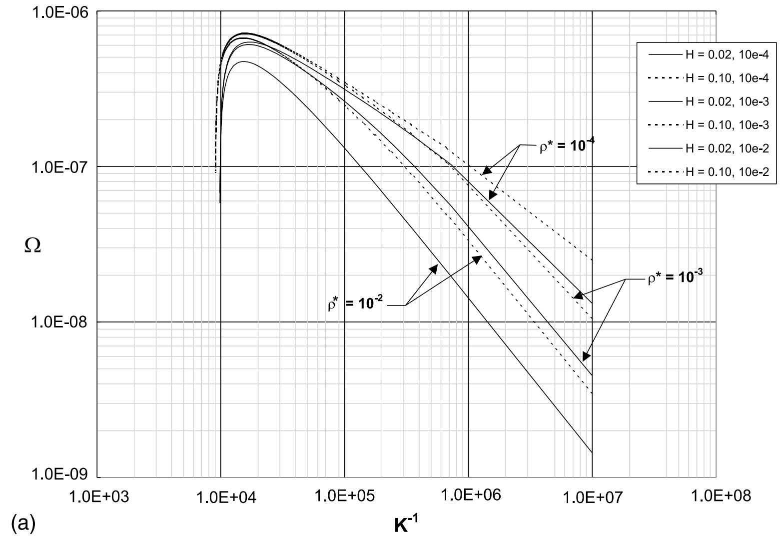

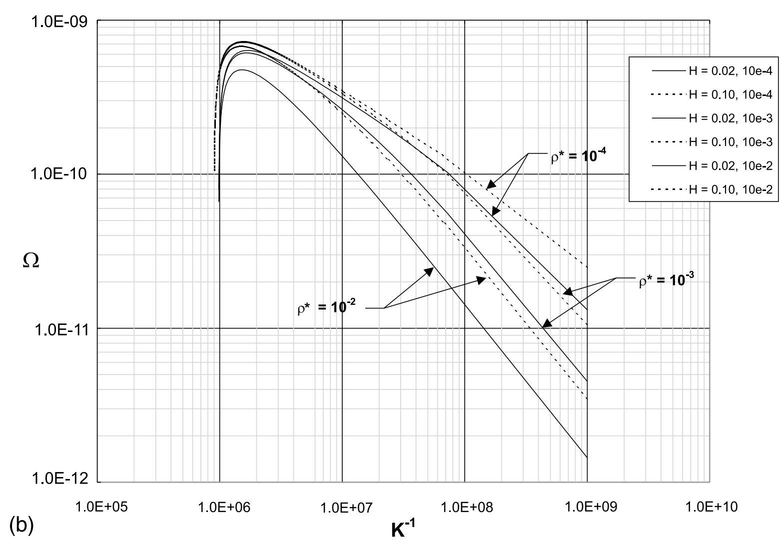

Fig. 6. Parametric solution of Eq. (25): (a) $R^* = 10^4$ (b) $R^* = 10^6$.

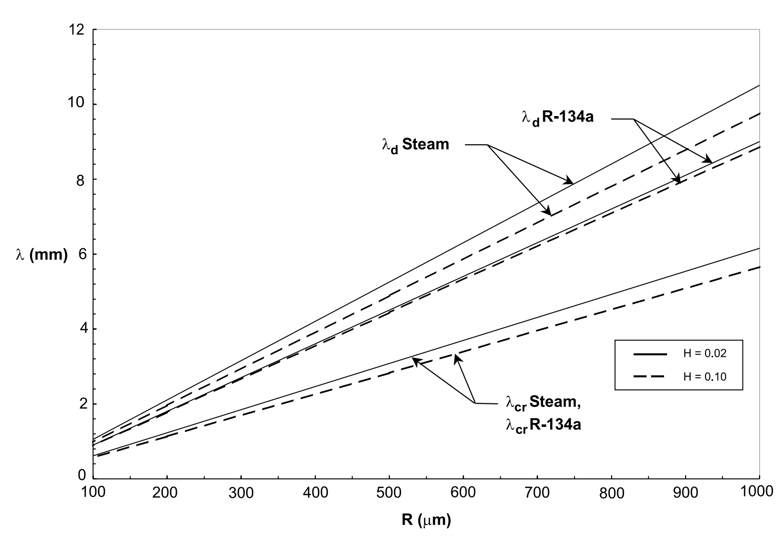

Fig. 7. Neutral and fastest growing wavelengths for saturated water-steam mixture at 1.0 MPa, and saturated R-134a liquid–vapor mixture at 1.017 MPa.

respectively, which cover the range of interest for microtubes with $R \approx 0.1$–1 mm subject to the flow of common fluids. Within the parameter range of interest, the solutions are evidently sensitive to R^* and ρ^*, and H. The fastest growing wave numbers are represented by the maxima on the displayed curves, while neutral waves occur when $\Omega = 0$. The flow field is thus generally unstable, due to the destabilizing effect of surface tension.

Wave numbers representing the neutral and fastest growing disturbances are of particular interest due to their potential role in boiling. Flow instability, furthermore, results in the formation of slugs that are of the order of magnitude of the fastest growing wavelength. Some parametric calculation results are shown in Fig. 7 for microtubes carrying saturated water and R-134a liquid–vapor mixtures at 1 bar pressure. The dimensionless neutral wavelength, λ_{cr}/R, as pointed out earlier, is the Rayleigh wavelength, Eq. (19). Parametric calculations show that λ_d is only a weak function of the liquid viscosity, and is of the same order of magnitude as λ_{cr}.

4. Concluding remarks

Linear stability of creeping inverted-annular gas–liquid flow in microtubes, when buoyancy is suppressed by surface tension, was analytically studied in this paper. Based on the stability solution of Hickox (1971), it was shown that the flow field is unstable with respect to long wavelength disturbances. For the limiting condition of zero phasic velocities a dispersion relation was derived based on a linear-stability analysis that accounted for the effect of viscosity, and was used in parametric calculations. The neutral wavelength coincides with the prediction of the Kelvin–Helmholtz stability theory.

Validation of the analytical results against experiments was not possible due to the unavailability of relevant experimental data. Experiments aimed at the elucidation of the characteristics of interfacial waves and their stability in microchannels are recommended.

References

Aul, R.W., Olbricht, W.L., 1990. Stability of a thin annular film in pressure-driven, low-Reynolds-number flow through a capillary. J. Fluid Mech. 215, 585–599.

Boomkamp, P.A.M., Miesen, R.H.M., 1997. Classification of instabilities in parallel two-pass flow. Int. J. Multiphase Flow 22, 67–88.

DeJarlais, G., 1983. An experimental study of inverted annular flow hydrodynamics utilizing an adiabatic simulation, US Nuclear Regulatory Commission Report NUREG/CR-3339, Washington, DC.

Dhir, V.K., Lienhard, J.H., 1973. Taylor stability of viscous fluids with application to film boiling. Int. J. Heat Mass Transf. 16, 2097–2109.

Frenkel, A.L., Babchin, A.J., Levich, B.G., Shlang, T., Sivashinsky, G.I., 1987. Annular flows can keep unstable films from breakup: Nonlinear saturation of capillary instability. J. Colloid Interfacial Sci. 115, 225–233.

Gauglitz, P.A., Radke, C.J., 1988. An extended evolution equation for liquid film breakup in cylindrical capillaries. Chem. Eng. Sci. 43, 1457–1465.

Ghiaasiaan, S.M., Abdel-Khalik, S.I., 2001. Two-phase flow in microchannels. Adv. Heat Transf. 34, 145–254.

Hickox, C.E., 1971. Instability due to viscosity and density stratification in axisymmetric pipe flow. Phys. Fluids 14, 251–262.

Hu, H.H., Joseph, D.D., 1989. Lubricated piping: Stability of core-annular flow, Part 2. J. Fluid Mech. 205, 359–396.

Joseph, D.D., Renardy, M., Renardy, Y., 1984. Instability of the flow of two immiscible liquids with different viscosities in a pipe. J. Fluid Mech. 141, 309–317.

Joseph, D.D., Renardy, Y., 1993. Fundamentals of two-fluid dynamics, Part II: Lubricated transport drops and miscible fluids. Springer, New York.

Kawaji, M., Banerjee, S., 1987. Application of a multifield model to reflooding of a hot vertical tube: Part 1—Model structure and interfacial phenomena. J. Heat Transf. 109, 204–211.

Kerchman, V., 1995. Strongly nonlinear interfacial dynamics in core-annular flows. J. Fluid Mech. 290, 131–166.

Lamb, S.H., 1932. Hydrodynamics. Cambridge University Press, Cambridge, UK.

Levich, V.G., 1962. Physiochemical hydrodynamics. Prentice Hall, Englewood Cliffs, New Jersey.

Li, J., Renardy, Y., 1999. Direct simulation of unsteady axisymmetric core-annular flow with high viscosity ratio. J. Fluid Mech. 391, 123–149.

Lin, C.C., 1955. The theory of hydrodynamic stability. Cambridge University Press, London, UK.

Preziosi, L., Chen, K., Joseph, D.D., 1989. Lubricated piping: Stability of core-annular flow. J. Fluid Mech. 201, 323–356.

Suo, M., Griffith, P., 1964. Two-phase flow in capillary tubes. J. Basic Eng. 86, 576–582.

Yih, C.S., 1967. Instability due to viscosity stratification. J. Fluid Mech. 27, 337–352.